Tomographic imaging of the ionospheric structure and disturbances in the East-Central Africa region

M Mutale[1], P Sibanda[1],

[1]Department of Physics, School of Natural Sciences, University of Zambia, Great East Road Campus, P.O Box 32379, Lusaka 10101, Zambia

E-mail: mubela.m@gmail.com

Abstract. Knowledge of the ionospheric electron density distribution and its fluctuations are essential for models such as the International Reference Ionosphere (IRI) for predicting ionospheric characteristics for radio wave propagation and for other applications such as satellite tracking and navigation. The Global Navigation Satellite Systems (GNSS), such as the Global Positioning System (GPS), can be used to determine the Total Electron Content (TEC) in the ionosphere. TEC is an important characteristic of the Earth's ionosphere that carries information on time and position variability of the ionosphere and has proved to be useful as a sensor of ionospheric climatology. However, such satellite to ground-based receiver measurements can only produce information about the density in the form of path-integrated snap-shots of the TEC. The challenge is to decompose its integral properly in the different values of electron density (Ne) in order to generate the distribution of the Ne with altitude. In this study, we use tomographic reconstruction techniques to successfully reconstruct altitudinal structure of the ionosphere from TEC data. Using the data from the recently installed Africa Array GPS stations in the central-Southern Africa region, we calculate three-hour average Ne profiles over this wide region using ionospheric tomography. The advantage of tomographic ionospheric Ne profiles is that they provide information of the Ne distribution up to global positioning system (GPS) orbiting altitude (with the coordination of space-based GPS tomographic profiles), and can be incorporated into the next generation of the IRI model. Since it uses real measurement data, tomographic average Ne profiles describe the ionosphere during quiet and disturbed periods.

1. Introduction

Because of the wide application of the ionosphere in space science, knowledge of the ionospheric vertical electron density (Ne) distribution is essential. Several factors affect the vertical distribution of the Ne, for example, solar activity such as flares and coronal mass ejections often produce large variations in the particle and electromagnetic radiation incident upon the earth. Such variations can, in turn, lead to disturbances of the magnetosphere. Such disturbances tend to generate large disturbances in ionospheric density distribution, total electron content (TEC), and the ionospheric current system. These ionospheric disturbances have important terrestrial consequences such as disrupting satellite communications and interrupting the flow of electrical energy over power grids. Furthermore, irregularly structured ionospheric regions can cause diffraction and scattering of trans-ionospheric radio signals. When received at an antenna, these signals present random temporal fluctuations in both amplitude and phase. This is known as ionospheric scintillation. Ionospheric scintillation may cause problems such as signal power fading, phase cycle slips, receiver loss of lock, etc., and degrade the quality of satellite navigation systems.

It is therefore necessary to obtain knowledge of the ionosphere as this is a natural resource for radio wave propagation. Knowledge of the ionospheric variations is essential in other aspects such as for error correction of Global Positioning System (GPS) applications, over the horizon radar, navigation, surveying, geodesy, and simplification of scientific research for Sun-Earth physicists.

Ionospheric tomography, proposed by Austen et al. (1986), has developed from initial modelling studies to be a viable technique for monitoring ionospheric Ne profiles. The first experimental results were presented by Andreeva et al. (1990), while Pryse and Kersley (1992) presented the first observation in which a tomographic Ne profile was verified by incoherent scatter radar (ISR). Several experimental campaigns have been conducted since then (e.g., Raymund et al., 1993; Foster et al., 1994; Kunitake et al., 1995; Mitchell et al., 1997; Yin et al., 2004; Yizengaw et al., 2004, and the references therein). These studies have extensively validated the performance of tomographic reconstruction technique in providing accurate Ne profiles of the ionosphere. However, all of these experimental campaigns were focused on extracting instantaneous or a few minute average Ne profiles using ground-based tomographic reconstruction of the slant total electron content (STEC). Therefore, tomography was not used to make average Ne profiles.

Although ionospheric tomography has been introduced to provide broad spatial coverage of ionospheric density profiles, most previous tomographic campaigns were focused on determining instantaneous Ne profiles. Currently, there are not sufficient densities of ionosonde or ISR facilities to make routine regional or global ionospheric Ne profiles. Therefore, global ionospheric models are used to “fill in” gaps in data coverage.

Currently, there are several models that provide a monthly mean value of ionospheric Ne distributions over an extended region of latitudes. Among these ionospheric models is the international reference ionosphere model which is one of the most widely used. However, calculating the average Ne over an extended region of latitude from real measurements has been restricted to areas where ground-based ionosonde and ISR facilities are located. Therefore, average Ne profiles in areas where those instruments are not available are needed to develop and test model Ne profiles.

This study uses a technique that can be used to calculate average Ne profiles over a wide area of coverage, using total electron content measurements from ground-based GPS receivers. The advantage of using GPS-TEC for such applications is they have a relatively low cost of installation and therefore there are dense networks of GPS receivers. The global distribution of GPS receivers is much denser than ionosondes and ISR. In this study we apply the tomographic reconstruction technique using GPS-TEC to calculate 3-hour average Ne profiles over a wide region within the central African region and show how the ionospheric electron density distribution varies with geomagnetic activity.

2. Data and method

The GPS constellation currently consists of 29 satellites orbiting at ~55° inclination in six distinct orbital planes and at ~20,200km altitude. Each satellite broadcasts two L-band signals at frequencies f_1=1.57542 GHz and f_2=1.2276 GHz. Owing to the dispersive nature of the ionosphere, dual frequency GPS measurements can provide integral information about the ionosphere and plasmasphere by computing the differential phases of the code and carrier phase measurements recorded at the ground-based GPS receivers (Klobuchar, 1996). Also, Mannucci et al. (1998) developed a method of calculating TEC from these GPS observables.

For this study we use the algebraic reconstruction technique (ART) to invert the GPS STEC into two-dimensional (altitude and latitude) average density profiles.

With this we observe how the ionosphere behaves at different levels of geomagnetic disturbance. The level of geomagnetic disturbance is quantified by the Kp index. The scale of Kp index ranges from 0 to 9, with Kp = 0 indicating no geomagnetic disturbance and Kp = 9 indicating extreme geomagnetic disturbance. Three hour averaged TEC values are used to derive tomographic images for two levels of geomagnetic activity, relatively quiet (with kp<2) and relatively disturbed (with kp>5).

The density values for individual pixels are then obtained from all STECs traversed through each pixel. This provides an averaged two dimensional description of the ionospheric Ne distribution. The images show how the level of geomagnetic activity as indicated by the Kp index affects the structure of the ionosphere.

The effectiveness of tomographic reconstruction depends on the distribution of the measurements. The International GNSS service (IGS) and the Africa Reference Frame (AFREF) and the Africa Array Networks have been set up and tomography has become a viable technique for ionospheric investigation in the African sector. Other GPS receiver networks have been set up in other locations such as the recently installed GPS stations is Zambia. These have created a relatively dense network for ionospheric tomography.

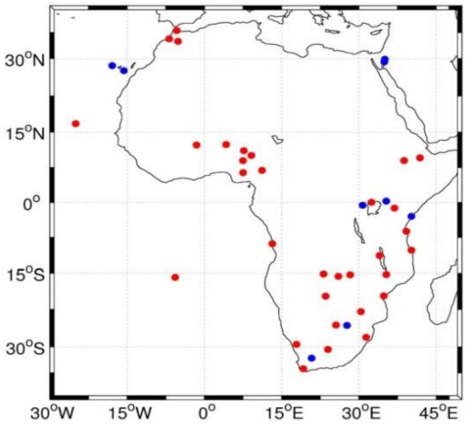

Figure1. Africa GNSS reference receiver stations

The results presented in this paper are obtained from measurements made during experimental campaigns using GPS stations in the East-Central African region.

Table 1: Geographical locations of the GPS stations being used in this study

Country	**GPS station name**	**Latitude**	**Longitude**
Zambia	Zamb	-15.42	+28.31
Zambia	Mong	-15.25	+23.15
Zambia	Tezi	-15.73	+26.02
Malawi	Mzuz	-11.43	+34.01
Kenya	Maua	-19.90	+23.53
Congo	Ulub	-11.63	+27.48
Tanzania	Dodm	-6.19	+35.75
	Zomb	-15.38	+35.33

3. Results

Although we have presented the 3-hour models for only two days, we have extensively analysed several case studies with similar respective levels of geomagnetic activities. Figure 2 presents results for a relatively "quiet day". The figure shows a gradual increase in ionization with very little disturbance in the structure of the ionization. On the other hand the "disturbed day" on Figure 3 although showing similar evolution in ionization has a lot more structure. Using the colour code, in figure 2a it can be seen that the level of ionization is very low at midnight as expected. The level of ionisation stays low for the rest of the night time hours because ionisation is mainly caused by solar radiation incident upon the earth which is not present at this time. The opposite is seen in the day time images (e.g. figure 2f and figure 3d) where the level of ionisation begins to increase with time. More so, the altitude over which there is ionization becomes wider. This is because the F1 and F2 layers become one layer at night and split into two during the day. Structure and density of the F region depend on the time of day and the zenith angle of the sun. Ionization density of the F1 layer depends on the zenith angle of the sun. The low ionization at night is also because the D layer is a daytime layer and therefore disappears at night. This layer accounts for the extension of the ionosphere to lower altitudes in the daytime images as well as the reduction during the night time images.

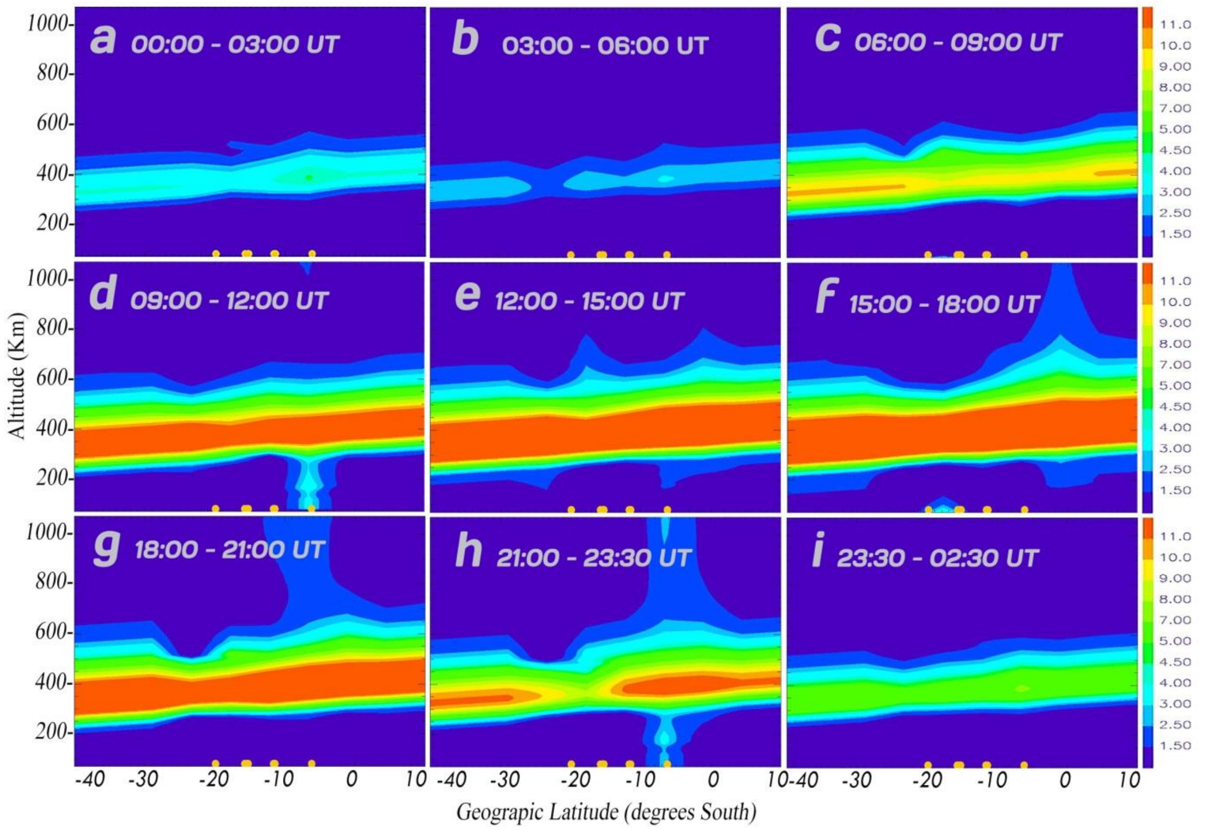

Figure 2. image of ionization on February 18 (Quiet day), showing the ionization on a graph of altitude against latitude. The right hand color code scale shows the electron density from 1.5 $X10^5$ el/cm^3 to 11 x $10^5 el/cm^3$. Each image is formed by taking all the TEC in a single 3-hour period averaging it to form the single image. The evolution shows selected images from midnight to midnight.

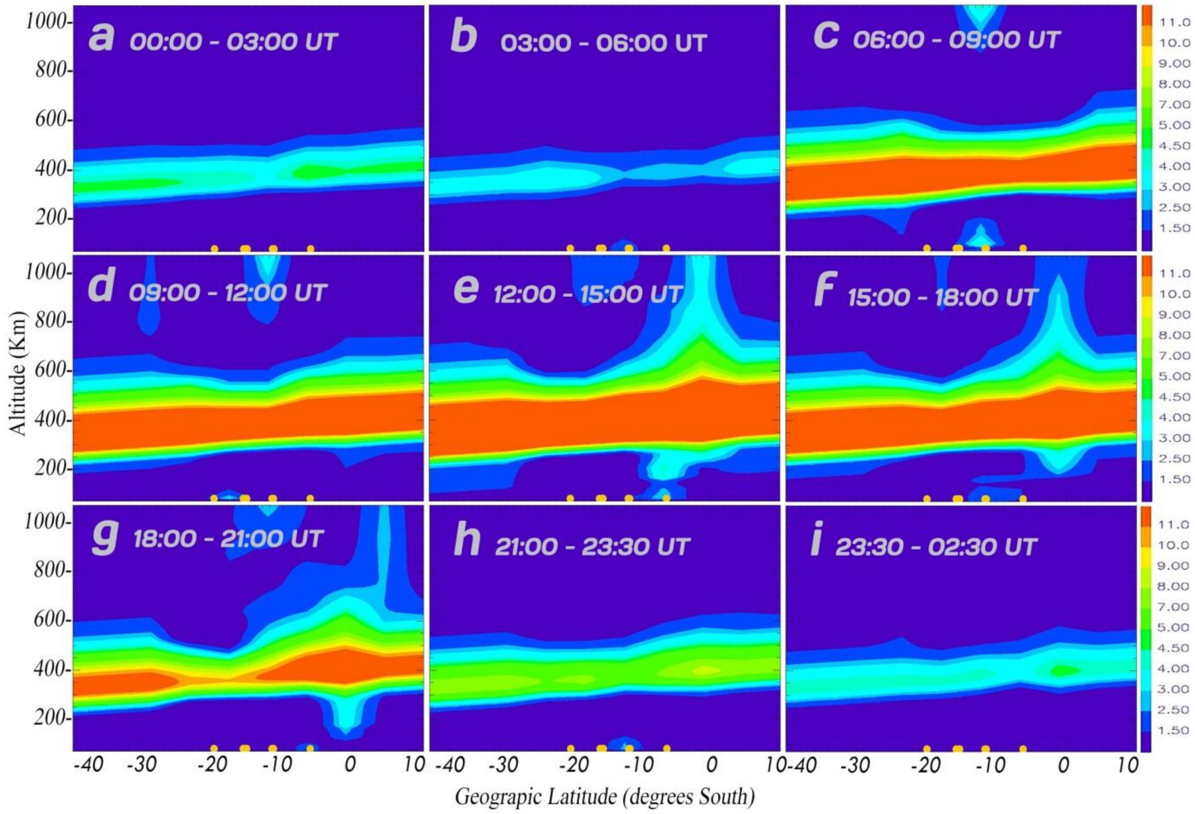

Figure 3. images showing the ionisation on March 9 (Disturbed day) – The images show how the evolution of ionisation due to diurnal changes occurs and how the ionisation levels are affected by geomagnetic disturbance. These are selected images showing the evolution from midnight to midnight. The left hand scale shows the altitude while the bottom scale shows latitude from equator going south. The right hand scale is a color coding for the electron density from 1.5 X 10^5el/cm^3 to 11 x 10^5el/cm^3.

At low latitudes the largest electron densities are found in peaks on either side of the magnetic equator; this is a feature known as the equatorial anomaly (figure 2c and 3a). The peak ionospheric concentrations do not occur on the equator, as might be expected from the maximum in solar ionizing radiation, but instead are displaced on either side. This anomaly occurs irrespective of day or season. The main driving force for the establishment of the equatorial anomaly (Fejar, 1991; Mikhailov et al, 1994) is the east west electric field, which is westward during night-time. Therefore, the corresponding resultant **E**×**B** motion is downward. This is opposite of that required to produce the anomaly; so such vertically extended density features would not normally be present at night.

Large scale structure such as the mid latitude trough (figures 2.h and 3.g), as well as a rise in ionization at the latitude 15°S geomagnetic in both the quiet and disturbed times are also present. Clearly the ionization during the disturbed period is a lot more evident and structured than the quiet period in day time as well as at night.

4. Conclusion

Although tomographically reconstructed density profiles have been extensively validated for the case of instantaneous Ne profiles and documented in for example, Raymund et al., 1993; Foster et al .,1994; Kunitake et al., 1997; Yin et al., 2004; Yizengaw et al., 2004, and the references therein, the tomographic profiles presented in this paper describe the averaged behaviour of the ionosphere. This knowledge is important to single-frequency GPS users who depend on ionospheric models to achieve optimal positioning accuracy because the ionospheric signal delay is the largest error source for positioning and navigation. Tomography provides Ne profiles at specific epoch owing to the fact that it uses calculated GPS-TEC. Though TEC is just an integrated parameter, ionospheric tomographic reconstruction routine using algebraic reconstruction enables us to decorelate this into the vertical distribution of the electron density profile thereby providing more information required for HF radio propagation. Other than that the technique used in this study shows how the level of geomagnetic activity affects the structure of the ionosphere. This is especially important for the topside ionosphere since current models have to rely on density profiles obtained from the sparsely located ground-based instruments that provide mainly bottom side Ne profiles to infer information about the topside ionosphere. The tomographic Ne profiles, which describe Ne distribution from ground to the GPS satellite altitude, can be used for the next generation of IRI models, enabling them to model the topside ionosphere more accurately. As long as dense arrays of GPS receivers are available, tomographic imaging can be used to augment sparsely located ground based instruments, such as ionosonde and incoherent scatter radar.

Acknowledgements
My gratitude goes to the University of Zambia for hosting this research. Also this research was supported by the Natural Science and Technological Council of Zambia NSTC. Thanks are due to the UNAVCO for the GPS data

References

[1] Andreeva E S, Galinov A V, Kunitsyn V E, Mel'nichenko Yu A, Tereshchenko E D, Filimonov M V and Chernykov S M 1990 *Journal of Experimematal and Theoretical Physics letter* **52**, 145 – 148.
[2] Austen J R, Fmake S J and Liu C H, 1986 In: Tauriainen A (Ed.), Radio Beacon Constributions to The Study of Ionization and Dynamics of The Ionosphere and to Corrections to Geodesy and Technical Workshop. *Ouluensis Universitas, Oulu, Finland*. 25-35.
[3] Bilitza D 2001 International reference ionosphere 2000 *Radio Science.* **36** 261-275.
[4] Fejer B G 1991 *Journal of Atmospheric and Terrestrial Physics.* **53** 677-693.
[5] Foster J C, Buonsanto M J, Klobuchar J A, Holt J M, Fougere P, Pakula W A, Raymund T D, Kuntisyn V E, Andreeva E S, Tereschenko E D and Kudukon B Z 1994 *International Journal of Imaging System and Technology*. **5** 148-159.
[6] Klobuchar J A 1996 Ionospheric effects on GPS. In: Parkinson B W and Spilker J J. (Eds). Global Positioning System: Theory And Application, vol. 1. *American Institute of Aeronautics and Astronautics INC.*
[7] Kunitake M, Ohtaka K, Maruyama T, Tokumaru M, Morioka A and Watanabe S 1995 *Annales Geophysicae,* **13** 1303-1310.
[8] Mikhailov A V, Förster M and Skoblin M G 1994 *Annales Geophysicae.* **12** 226-231.
[9] Pryse S E, Kersley L, 1992 *Journal of Atmospheric and Terrestrial Physics* **54** 1007-1012.
[10] Raymund T D, Pryse S E, Kersley L, Heaton J A T 1993 *Radio Science* **28** 811-818.
[11] Yisengaw E, Dyson P L, Essex E A and Moldwin M B 2005a *Annales Geophysicae* **23** 707-721.